Superconductivity 3 (2022) 100023

Contents lists available at ScienceDirect

Superconductivity

journal homepage: www.elsevier.com/locate/supcon

Performance of highly flexible sub-cable for REBCO Cable-In-Conduit conductor at 5.8 T applied field

Guanyu Xiao [a,b], Huan Jin [a,*], Chao Zhou [a], Hongjun Ma [a], Donghu Wang [a], Fang Liu [a], Huajun Liu [a], Arend Nijhuis [c], Arnaud Devred [d]

[a] Institute of Plasma Physics, Chinese Academy of Sciences, PO Box 1126, Hefei, Anhui 230031, China
[b] University of Science and Technology of China, No.96, JinZhai Road Baohe District, Hefei, Anhui 230026, China
[c] University of Twente, Faculty of Science and Technology, 7522 NB Enschede, The Netherlands
[d] European Organization for Nuclear Research (CERN), CH-1211 Geneva, Switzerland

ARTICLE INFO

Keywords:
REBCO
HFRC cable
CICC
Electromagnetic cycling
Performance degradation

ABSTRACT

Due to the high current capability and excellent flexibility, High Flexible REBCO Cables (HFRC) have emerged as an important candidate for composite high-temperature superconducting conductors. The REBCO six around one Cable-In-Conduit Conductor (CICC) concept has been designed for application in the Central Solenoid (CS) coil of the China Fusion Engineering Test Reactor. In the application of fusion devices, the performance of CICC under electromagnetic (EM) loading and thermal stress is very important for reliable and economic operation. Therefore, a 1.22 m long sub-cable with HFRC design for CICC was manufactured and tested at 4.2 K in a background magnetic field up to 5.8 T. The aim is to investigate the stability of the current-carrying properties of the HFRC cable under electromagnetic and thermal cyclic loading. The test results show that the critical current (I_c) of the HFRC cable reached 17.3 kA in a background magnetic field of 5.8 T at 4.2 K. Furthermore, no performance degradation was observed after 24 cycles of 80 kN/m peak load with a background field of 5.8 T and 8 warm-up-cool-down cycles between 77 K and room temperature. The test results provide a good basis for the development of full-size conductors in future magnet applications.

Introduction

The next generation of high-field magnets for fusion experiments and their Cable-In-Conduit Conductors (CICC) require high operating currents in magnetic fields exceeding 20 T [1,2]. The limitations of the upper high magnetic field, current density, and critical temperature on low-temperature superconductors (LTS) CICC warrant the development of cables manufactured from high-temperature superconductors (HTS) of REBCO and Bi2212 [2,3]. Compared to Bi-2212 round wires, REBCO coated tapes have high mechanical strength, high irreversibility field, extended commercial production, and no phase forming heat treatment [4–6].

To promote REBCO tapes for fusion high-filed magnets applications, it is necessary to use many REBCO tapes in parallel to manufacture a cable or CICC, to maximize current capacity, allow sufficient cooling, and provide structural support [7]. Several REBCO cable structures are considered for example: Roebel, twisted stack tape conductor (TSTC), conductor on a round core (CORC), and VIPER [7–9].

Based on the different REBCO cable concepts, researchers have developed a variety of REBCO CICC structures and conducted preliminary studies. The ENEA research group has proposed a design of a REBCO tapes-based CICC with TSTC cable on a slotted core and prototyped a short industry-ready Twisted-stack slotted core HTS CICC (TSTC HTS CICC) in 2014 [10,11]. The CICC consists of five stacks of 30 REBCO tapes each, an aluminum slotted core, and a round aluminum jacket, and has been tested at KIT, demonstrating a critical current of about ~9 kA at 4.2 K, in self-field[12]. The first CORC six-around-one CICC was proposed and manufactured for large-scale magnets by Advanced Conductor Technologies (ACT) and CERN in 2016 [13]. Three CORC-based CICCs for high current comprised six CORC cables in a six-around-one configuration in combination with a jacket and were tested in the SULTAN test facility [2,14]. The Central Solenoid (CS) magnet for the Chinese Fusion Engineering Test Reactor (CFETR) is expected to operate with a current higher than 45 kA at a magnetic field up to 17 T [15,16] and under AC operation. The inlet temperature of the CS magnet is 4.5 K. To meet the operational

* Corresponding author.
E-mail addresses: jinhuan@ipp.ac.cn, jinhuan@ipp.ac.cn (H. Jin).

https://doi.org/10.1016/j.supcon.2022.100023
Received 3 July 2022; Revised 30 August 2022; Accepted 31 August 2022
Available online 7 September 2022

requirements, one highly flexible REBCO (HFRC) cable design, derived from the CORC cable concept, has been proposed for a full-size CICC design by the Institute of Plasma Physics, Chinese Academy of Science (ASIPP), as shown in Fig. 1.

Electromagnetic and thermal cycling are important experiments to evaluate the operational stability of CICC cables and generate transverse and longitudinal compression loads of the strands in the cable. Lots of related research works have been performed on low-temperature superconductors (LTS) CICC cables for fusion application. In 2003, the strain state of Nb3Sn strands was analyzed by finite element model simulation of Nb3Sn CICC cables, showing that transverse loads cause bending strains in the Nb3Sn strands, leading to a degradation in the Ic and n-value of CICC cables [17]. In 2013, the test results of Nb3Sn CICC SULTAN samples were analyzed. Due to the transverse loads, the final equilibrium position of Nb3Sn strands is reached after friction and several thermal cycling, which change the strain state of Nb3Sn strands, leading to a reversible decrease in the Ic [18,19]. A comprehensive analysis of the impact of EM and thermal cycles at different operating conditions on the performance of the Nb3Sn CICCs of the ITER magnet system was reported in 2021[20]. The rate of conductor Ic degradation increase with the applied EM loads and the warm-up-cool-down (WUCD) cycles have a predominant effect on the TF conductor performance.

A 1.22 m long HFRC cable of REBCO CIC-conductors was manufactured by an industrial process and tested in self-field at 77 K with a background magnetic field of 5.8 T at 4.2 K. In total 36 REBCO tapes from Fujikura were wound into 13 layers around a spiraled tube, to form the HFRC cable (see Fig. 1). The HFRC cable was inserted into a round stainless steel jacket. The design aim is a performance of 15 kA at 4.2 K, 5.8 T and to verify its stability during operation in a background magnetic field. The HFRC cable was subjected to EM cycling at different EM loads under a 5.8 T background field and WUCD cycles between 77 K and RT. The results provide an important basis for the design of REBCO superconducting magnets for future fusion devices.

EM and thermal cycling tests

Concept of HFRC cable design

As shown in Fig. 1(a), six sub-cables are spirally wound around a hollow tube and inserted into a square jacket to manufacture a REBCO CICC. The HFRC concept has been proposed by ASIPP and designed for the sub-cable of CICC [21]. Fig. 1(b) shows the structure of the HFRC cable. This internal spiraled tube in the cable provides better flexibility and cooling. Internal forced flow gas cooling of the CICC during operation can be directly through the perforated tube, the gaps between adjacent pitches of the central spiral tube, and the gaps between adjacent wound tapes. To verify the performance of the sub-cable, the HFRC cable was inserted into a round jacket to provide mechanical support and protection during the experiment.

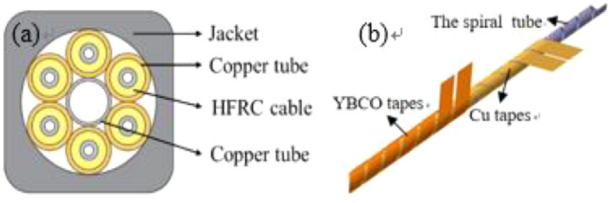

Fig. 1. (a) Schematic diagram of the REBCOCICC; (b) The concept of the HFRCcable.

The description of HFRC cable

The first HFRC cable is manufactured at ASIPP. The HFRC cable was manufactured with REBCO tapes purchased from Fujikura with a substrate thickness of 50 μm, the width, and thickness of the tapes are 4 and 0.1 mm, respectively. The used inner spiral tube has an outer diameter of 4.95 mm and a wall thickness is 0.5 mm. Its helical pitch is 8.6 mm. Since winding the REBCO tapes directly on the spiral tube would produce stress concentrations and could possibly cause damage to the tape, two layers of copper tapes with 4 mm width and 0.075 mm thickness were spirally wound around the spiral tube. This makes the HFRC core outside diameter around 5.25 mm. A 1.22 m long HFRC cable was wound in a mechanically well-controlled way from 36 REBCO tapes in 13 REBCO layers. The outer ten REBCO layers comprise 3 tapes each, and the inner three layers comprise 2 tapes each. In addition, seven layers of copper tape, 4 mm in width and 0.1 mm in thickness, were wound around the outer REBCO layer to provide flexible protection during the stainless steel jacket compaction.

Then the HFRC cable was inserted into a round stainless-steel tube. The used jacket has an outer diameter of 15 mm and a wall thickness of about 1.57 mm. The jacket tube diameter is reduced machine until its inner wall contacts the outermost layer of the HFRC cable. The outer diameter of the final jacket is 13.60 mm. More geometrical properties of the HFRC cable are summarized in Table 1. Fig. 2 shows the manufactured HFRC cable sample and the position of the voltage tap.

The HFRC cable joints were trimmed into a staircase and mounted in the U-shaped groove of the rectangular terminal. The terminals are made of oxygen-free copper (OFC) plates with a length of 280 mm. A U-shape groove that matches the outer diameter of the cable was machined to match as the bottom plate. After assembly, the groove was fully filled with PbSnCd solder (melting point 145 ˚C) using a temperature of around 190 ˚C. The total terminal heating time was less than 10 min. An additional 50 mm long jacket tube support was connected to the upper plate to avoid mechanical damage to the root of the cable joints. Fig. 3 shows a schematic diagram of the structure of the CICC joint terminals.

Testing procedure for HFRC cable

The test facility consists of a cryostat, a superconducting transformer, a data acquisition system, a quench detection, and a protection system. As shown in Fig. 4, the test sample was connected to the superconducting transformer, which is able to provide an operating current of up to 30 kA. The background magnetic field was supplied by a NbTi superconducting dipole magnet with an 80 mm diameter bore at ASIPP, providing a transversal magnetic field up to 5.8 T on the HFRC cable, as shown in Fig. 4. The sample is inserted vertically into the bore of the superconducting magnet. Due to the size limitation of the test facility, the central magnetic field of the background magnet is close to the bottom joint terminal of the HFRC cable. For testing, the cable is immersed in liquid helium.

Table 1
The main parameters of the HFRC cable with jacket.

Parameters	Value
Number of REBCO tapes	36
Number of layers	13
Number of copper tapes	25
Central core OD (mm)	5.25
HFRC OD (mm)	10.40
Length (m)	1.22
Jacket tube OD (mm)	15
CICC OD (mm)	13.60
CICC jacket length (mm)	660

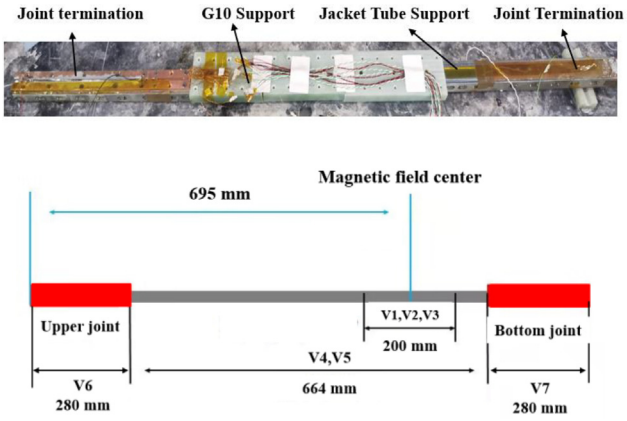

Fig. 2. Photograph of the manufactured HFRC cable with jacket layout and the position of the voltage tap.

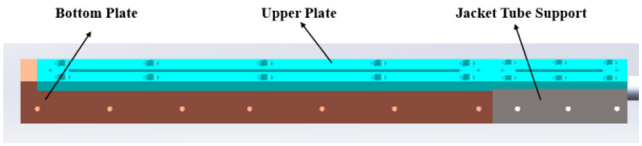

Fig. 3. A schematic diagram showing the HFRC cable joint terminations.

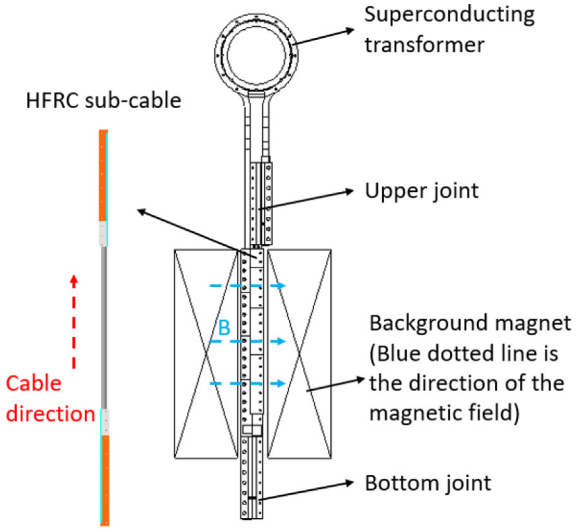

Fig. 4. Schematic diagram of the structure of the conductor test facility.

The prepared HFRC cable was then subjected to critical current and EM cycling tests with different electromagnetic loads at 4.2 K and 5.8 T. Then, to study the effect of thermal stress cycling on the HFRC cable, it was disassembled from the superconducting transformer. Subsequently, it was subjected to WUCD cycling tests, carried out between 77 K and RT by dipping the sample in liquid nitrogen, warming it to RT, and immersing it again in liquid nitrogen, and repeating this several times.

To monitor the current distribution in the outermost tape layers, three pairs of voltage taps were soldered to the three REBCO tapes in the outermost layers of the cable. Their positions are symmetrical about the magnetic field center of the background superconducting magnet. In addition, three pairs of voltage taps spaced by around 66 cm were soldered at the joint root to measure the voltage signal of the whole HFRC cable. One of them was connected to a quench detection and protection system, which was designed to activate the quench protection process when the voltage exceeds a pre-set value.

Results

Critical current tests

The voltage taps used to measure the voltage signal of the whole HFRC cable were used to evaluate, the critical current by using the recorded *V-I* characteristics. Fig. 5 shows the *V-I* characteristics of the HFRC cable at 77 K, self-field. The critical current was calculated by means of the following fitting equation from the measured voltage (V) as a function of the increased current (I):

$$V = V_c(I/I_c)^n + V_0 \quad (1)$$

where V_0 is the inductive offset voltage, n is a fitting parameter representing the steepness of the transition, and V_c is the critical current criterion of 1 μV/cm multiplied by the distance of the voltage taps. Based on this nonlinear fitting, the calculated Ic and n for the HFRC cable are 4211 A and 26.4 at 77 K, self-field, respectively.

Fig. 6 shows the *V-I* characteristics of the HFRC cable at 4.2 K with different background magnetic fields. The I_c was determined from the *V-I* curve at a criterion of 1 μV/cm, and the *n*-value is between 0.1 to 1 μV/cm. When the background magnetic field increased from 5 to 5.8 T, the measured Ic and *n*-value changed from 18.4 to 17.3 kA, and 26.8 to 24.1, respectively. The result of the electromagnetic analysis of a cable model (Fig. 7) shows a combined peak magnetic field of up to 6.3 T at a critical current of 17.3 kA.

Electromagnetic (EM) cycling and quenching

The critical current as a function of the number of electromagnetic cycles is shown in Fig. 8. Firstly, to verify the operational stability of the sample at low EM loads, 5 EM cycling tests were carried out with an operating current (I_{op}) of 10 kA, which is about 60% of the I_c. The I_c and *n*-value results showed that the performance of the HFRC cable was hardly affected. Then, to verify the operational stability of the sample at high EM loads, eight EM cycling tests were carried out with an I_{op} of 15 kA, which is about 90% of the I_c. The generated EM load is about 90 kN/m, and the I_c gradually decreased to 14.5 kA, which is less than the I_{op} of 15 kA. Compared to the initial critical current of 17.3 kA, the I_c is reduced by about 16%. In order to avoid sample quench, the I_{op} in the EM cycles needs to be reduced and the EM loads need to be lowered. Therefore, for the next 27 EM cycles, the I_{op} was decreased to 13.1 kA, which is 90% of the I_c of 14.5 kA. The EM load was reduced to about 80 kN/m. The I_c rapidly decreased during the first three cycles down to 13.7 ± 0.1 kA, and after that, no significant I_c degradation was observed along 24 EM cycles. The small fluctuation

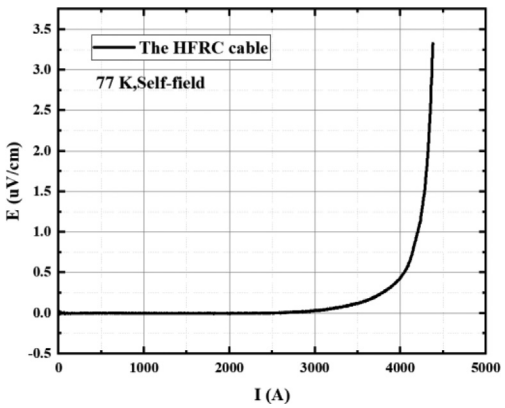

Fig. 5. The *V-I* characteristics of the testing sample at 77 K, self-field.

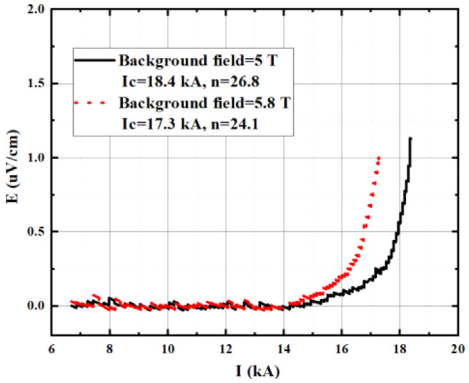

Fig. 6. The *V-I* characteristics of the testing sample at 4.2 K and different background magnetic fields.

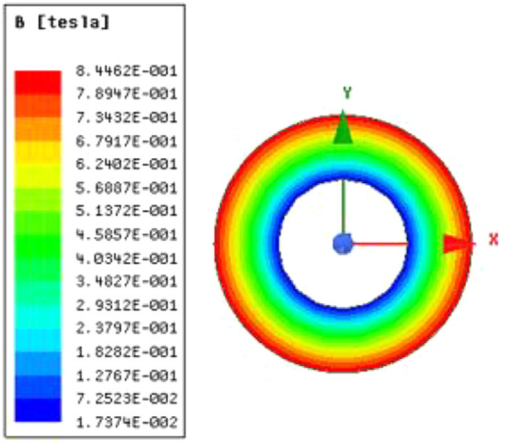

Fig. 7. Self-field distribution of the cable with 25 kA operating current.

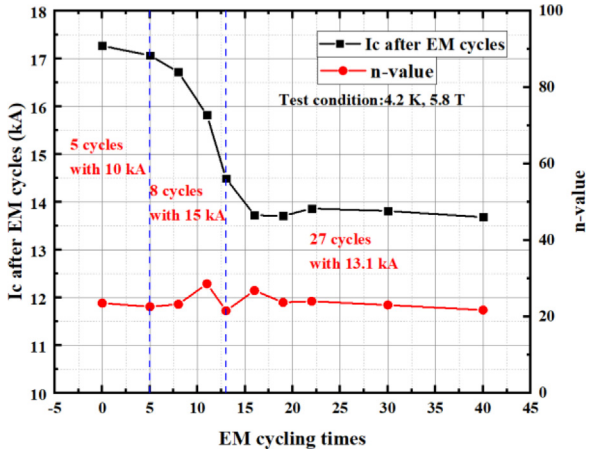

Fig. 8. Testing sample electromagnetic cycling results.

observed for the critical current and *n*-value may partly have been caused by varying current sharing conditions by settling of the wound tapes in the HFRC cable.

The experimental results show that the maximum EM load that the HFRC cable can withstand for cycling is about 80 kN/m. The decrease in the critical current may be caused by damage to the REBCO layers in the tapes from the HFRC cable. This is further explored in Section 4, by implementing the HFRC cable disassembly procedure, in order to carry out experiments to verify the performance of the individual REBCO tapes in the cable.

The HFRC sample experienced two quenches after EM cycling. The operating current in excess of the I_c is injected into the HFRC sample, resulting in a rising potential, and triggering the quench protection of the sample. After quench, the I_c was reduced to 12.2 kA, and the n-value was 17.7. It was observed that the cable sample experienced about an 11% decrease in current carrying performance after two quenches. It is most likely caused by the local thermal stress concentrations during quenching.

Warm-up-cool-down (WUCD) cycling

After EM cycling and quench, significant degradation in the critical current of the HFRC sample occurred. In order to investigate whether the current carrying performance of the damaged cable samples would be further degraded under thermal stress, a total of 8 WUCD cycle tests between 77 K and RT were carried out. The sample was disassembled from the superconducting transformer before conducting the WUCDs experiments. After the sample was disassembled from the test facility, it was tested at 77 K and self-field. The calculated Ic and n-value for the HFRC cable are 1647 A and 4, respectively. Compared with the initial current of 4211A, the I_c is decreased by about 62%, and the n-value is significantly lower. It indicates that the REBCO tapes wound on the HFRC cable were damaged. It is most likely caused by the EM loads, thermal stress from the quench, and mechanical stress from the disassembly process of the test facility.

The calculated I_c and *n*-values at 77 K for all 8 thermal cycling tests are shown in Fig. 9. The I_c of the HFRC cable along the WUCD cycling tests were all in the range of 1617 ± 30 A at 77 K and in self-field. The *n*-value determined within the electric field interval from 0.1 to 1 μV/cm was 5 ± 0.4. The I_c and *n*-value did not further decrease during the 8 WUCD cycles. In addition, it is observed that the application of stress, whether it is by means of EM or WUCD, can bring small changes in the current sharing conditions between the REBCO tapes, which on its turn can introduce small fluctuations in the measured I_c and *n*-value.

Discussion

To investigate the possible reasons for the significant degradation in performance of the HFRC cable, it was disassembled. The outer round stainless steel jacket was carefully cut with a milling cutter. The REBCO tapes were disassembled layer by layer and numbered sequentially from the outside to the inside. As illustrated in Fig. 10,

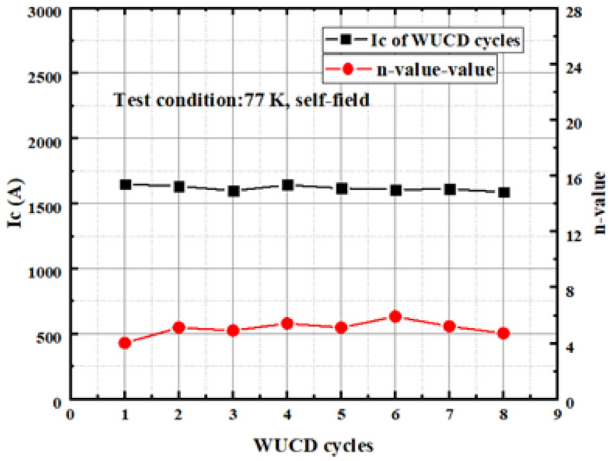

Fig. 9. The measured I_c and *n*-value during thermal cycling at 77 K, self-field.

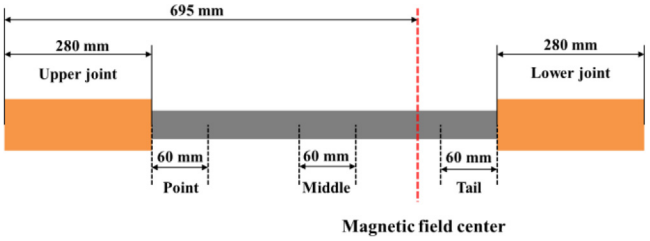

Fig. 10. Sampling layout of disassembled REBCO tapes.

sections of REBCO tape at the point, middle, and tail of the HFRC cable were selected to carry out critical current tests at 77 K, in self-field. The test was carried out with the four-point measurement method. The critical currents of the selected samples are shown in Fig. 11. Fig. 12 shows clear scratches on the inside of some of the poorly performing disassembled samples. These scratches may be caused by the extrusion and slippage of adjacent layers under EM stress. EM stress results in certain degradation to the critical current of the outer tapes. The test results show that specifically the tapes at the tail of the HFRC cable were damaged up to a certain extent. The likely reason is that the tail of the HFRC cable is closer to the center of the background magnetic field and is subjected to the largest EM load.

In addition to the damage near the lower joint, the mechanical strength of the inner spiral tube of the HFRC cable may be one of the important factors for the degradation of the cable's current-carrying capacity. The effect of transverse compressive load on the spiral tube has been investigated at room temperature (RT). The spiral tube is placed between two flat anvils that can be compressed, as shown in Fig. 13. The top anvil diameter is 65 mm and attached to a servohydraulic actuator. The transverse mechanical performance of only the spiral is shown in Fig. 14. The radial compressive deformation of the spiral is about 0.6 mm at a transverse load of 85 kN/m. At this point, the spiral tube gradually changes from elastic to plastic deformation, creating increased strain concentrations in the REBCO tapes. This is a likely explanation for the degradation of the critical currents of the disassembled tapes. Note that especially the outer tapes suffered the most from the EM loading.

To improve the EM loading capacity for the HFRC cable of REBCO CICC, the structural parameters of the inner spiral tube will be redesigned to meet the mechanical strength and flexibility requirements. The protective structure will also be optimized to give reliable support

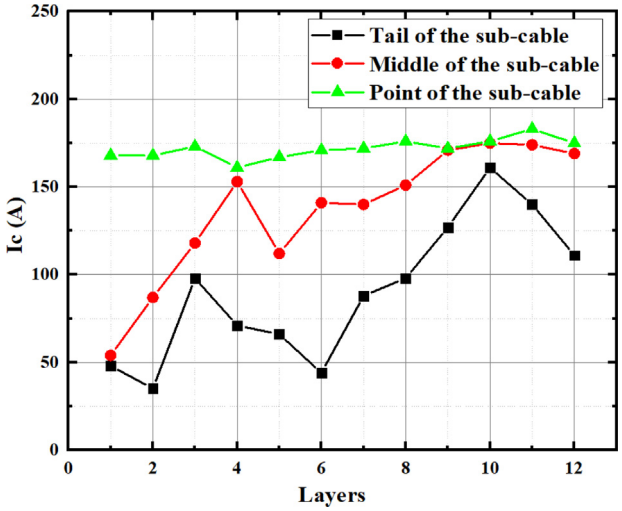

Fig. 11. Disassembled the wound REBCO tapes critical current tested results.

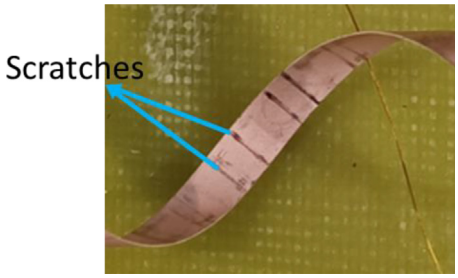

Fig. 12. The disassembled tape.

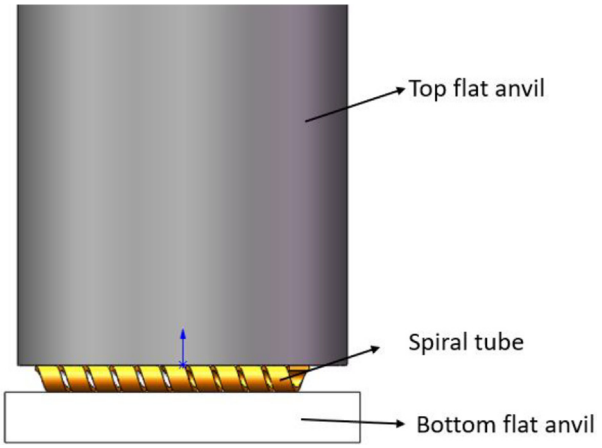

Fig. 13. Schematic diagram of the spiral located on the transverse compressive test facility.

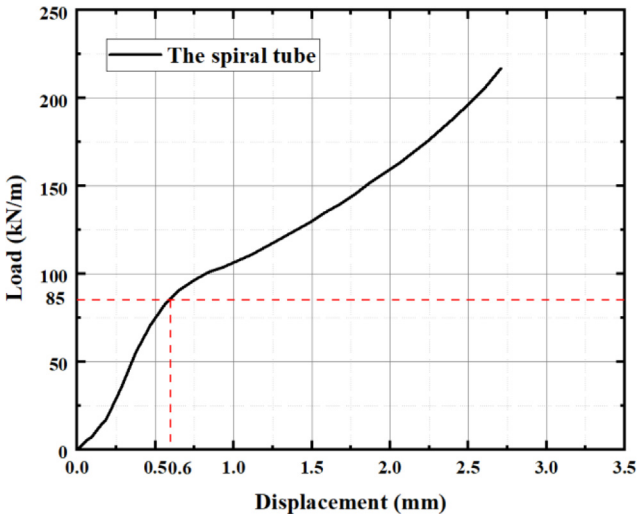

Fig. 14. The transverse mechanical performance of the spiral tube.

and protection to the root of the HFRC cable joint subjected to high EM loads in the next step.

Conclusions

The first long sub-cable with HFRC design contains 36 REBCO tapes with a width of 4 mm and a substrate thickness of 50 μm. It was designed to operate in a magnetic field of up to 5.8 T to address key challenges in the manufacturing and application of REBCO CICC. The critical current and *n*-value of the HFRC cable are 4211 A and

26.4 respectively, measured at 77 K and in self-field. When the background magnetic field increased from 5 T to 5.8 T, the measured I_c and n-value changed from 18.4 to 17.3 kA, and the n-value from 26.8 to 24.1. In total 40 EM cycling and 8 WUCD tests were applied to the HFRC cable to demonstrate the impact of EM and thermal loads. The changed stress and strain conditions may cause variation in the current sharing conditions between the REBCO tapes. The critical current of the HFRC cable was decreased by 15% after 8 EM cycles of about 90 kN/m. Then, a stable critical current of 13.7 ± 0.1 kA was reached, at 4.2 K, and a background field of 5.8 T, after 24 EM cycles of 80 kN/m loads. The degradation of the HFRC cable after EM cycles is mainly caused by the poor mechanical strength of the central spiral tube. At 77 K and self-field, the I_c of the HFRC cable during 8 WUCD cycles remained in the range of 1617 ± 30 A, and no degradation was observed during thermal cycles. These results will provide important guidelines for the design of a full-size REBCO CICC in the future. Because of the strain-sensitive characteristics of YBCO tapes, stress concentrations in the REBCO tapes should be avoided during cable winding and manufacturing. Additional mechanical damage should be avoided during the cable test facility assembly process. The EM load performance of the cable depends mainly on the structural design of the cable and the mechanical strength of the core material. Optimizing the cable structure and enhancing the mechanical strength of the spiral tube may help improve the EM load performance of the HFRC subcable. A new sample with a new spiral tube will be prepared, and the results will be reported in the future.

Declaration of Competing Interest

The authors declare that they have no known competing financial interests or personal relationships that could have appeared to influence the work reported in this paper.

Acknowledgments

This work is supported by the National Key R&D Program of China (No. 2022YFE03150200), the Strategic Priority Research Program of Chinese Academy of Science under Grant No.XDB25000000, Comprehensive Research Facility for Fusion Technology Program of China under Contract No.2018-000052-73-01-001228, the National Nature Science Foundation of China (No. 52077212), and the Youth Innovation Promotion Association, Chinese Academy of Science (Grant No.2021444).

References

[1] Rossi L, Badel A, Bajko M. The EuCARD-2 future magnets European collaboration for accelerator-quality HTS magnets. IEEE Trans Appl Supercond 2015;25(3):4001007.
[2] Weiss JD, Mulder T, et al. Introduction of CORC wires: highly flexible, round high-temperature superconducting wires for magnet and power transmission applications. Supercond Sci Technol 2017;30(1):014002.
[3] Zhang Y, Hazelton D W, Kelly R, et al. Stree-Strain Relationship, Critical Strain (Stress) and Irreversible Strain (Stress) of IBAD-MOCVD-Based 2G HTS Wires Under Uniaxial Tension. IEEE Trans Appl Supercond 26;4, 840040.
[4] Mulder T, Dudarev A, Mentink M, et al. Performance test of an 8 kA @ 10 T 4.2 K REBCO-CORC cable. IEEE Trans Appl Supercond 2016;26(4):4803705.
[5] Goldacker W, Grilli F, Pardo E, et al. Roebel cables from REBCO coated conductors: a one-century-old concept for the superconductivity of the future. Supercond Sci Technol 2014;27(9):093001.
[6] Obradors X, Puig T. Coated conductors for power applications: materials challenges. Supercond. Sci. Technol. 27;4, 044003.
[7] Hartwing Z S, et al. 2020 Supercond. Sci. Technol. 33 11LT01.
[8] Takayasu M, Chiesa L, Bromberg L, Minervini JV. Cabling method for high current conductors made of HTS tapes. IEEE Trans Appl Supercond 21:4, 2340-4.
[9] Laan DCVD. Effect of a compressive uniaxial strain on the critical current density of grain boundaries in superconducting YBCO. Supercond Sci Technol 2009;22:065013.
[10] Gelentano G, Marzi GD, Fabbri F, et al. Design of an industrially feasible twisted-stack HTS Cable-in-Conduit conductor for fusion application. IEEE Trans Appl Supercond 2014;24(3):4601805.
[11] Marzi GD, Allen NC, Chiesa L, Celentano G, et al. Bending tests of HTS Cable-In-Conduit conductors for high-field magnet applications. IEEE Trans Appl Supercond 2016;26(4):4801607.
[12] Muzzi L, Marzi GD, Zenobio AD, Corte AD. Cable-in-conduit conductors: lessons from the recent past for future developments with low and high temperature superconductors. Supercond Sci Technol 2015;28(5):053001.
[13] Mulder T, Dudarev A, Mentink M, Silva H. Design and manufacturing of a 45 kA at 10 T REBCO-CORC Cable-in-Conduit conductor for large-scale magnets. IEEE Trans Appl Supercond 2016;26(4):4803605.
[14] Mulder T, Weiss JD, Laan DVD, Dudarev A, Kate HHJT. Recent progress in the development of CORC Cable-In-Conduit conductors. IEEE Trans Appl Supercond 2020;30(4):4800605.
[15] Ma Y, Wu Y, et al. Conceptual Design of the Power Supply System for the CFETR CS model coil. IEEE Trans Appl Supercond 2018;28(5):4204405.
[16] Godeke A, Cheng D, Dietderich DR, et al. Limits of NbTi and Nb3Sn, and development of W&R Bi-2212 high field accelerator magnets. IEEE Trans Appl Supercond 2007;17(2):1149–52.
[17] Mitchell N, Devred A, Larbalestier DC, Lee PJ, Sanabria C, Nijhuis A. Reversible and irreversible mechanical effects in real cable-in-conduit conductors. Supercond Sci Technol 2013;26:114004.
[18] Calzolaio C, Bruzzone P, Stepanov B. Monitoring of the thermal strain distribution in CICCs during the cyclic loading tests in SULTAN. IEEE Trans. Appl. Supercond. 2013;23:4200404.
[19] Breschi M et al. Impact of mechanical and thermal cycles at different operating conditions on the ITER toroidal field coil conductor performance. Supercond. Sci. Technol. 2021;34(8):085021.
[20] Mitchell N. Mechanical and magnetic load effects in Nb3Sn cable-in-conduit conductors. Cryogenics 2003;43(3–5):255–70.
[21] Guo ZC, Qin JG, et al. AC loss and contact resistance in highly flexible rebco cable for fusion applications. Superconductivity 2022;2:100013.